THE ASTROPHYSICAL JOURNAL, 344:715–725, 1989 September 15

PLANETARY NEBULAE AS STANDARD CANDLES. IV. A TEST IN THE LEO I GROUP

ROBIN CIARDULLO[1] AND GEORGE H. JACOBY[1]
Kitt Peak National Observatory, National Optical Astronomy Observatories
AND
HOLLAND C. FORD[1,2]
The Johns Hopkins University and Space Telescope Science Institute
Received 1988 December 28; accepted 1989 March 1

ABSTRACT

We present the results of a planetary nebula survey of galaxies in the Leo I group performed with the Kitt Peak and Cerro Tololo 4 m telescopes and on-band off-band λ5007 interference filters. In all, we detected 249 PN candidates populating the top 1.5 mag of the planetary nebula luminosity function (PNLF), including 93 in the E0 galaxy NGC 3379, 54 in the E6 galaxy NGC 3377, and 102 in the S0 spiral NGC 3384. In all three galaxies, the luminosity specific planetary nebula number densities are roughly the same, and the derived stellar death rates are in remarkable agreement with the predictions of stellar evolution theory.

Using statistically complete and homogeneous samples of planetaries, we show that the shape of the [O III] λ5007 planetary nebula luminosity function is the same in each galaxy and indistinguishable from that observed in M31 and M81. By comparing the PNLFs with an empirical law, we find the most likely distances to NGC 3377, 3379, and 3384 are 10.3, 9.8, and 10.1 Mpc, respectively, with formal 1 σ errors of $\sim$10%. This invariance in galaxies with differing Hubble types and metallicities demonstrates that the PNLF is an excellent standard candle for early-type galaxies.

Subject headings: galaxies: distances — galaxies: individual (NGC 3377, NGC 3379, NGC 3384) — galaxies: stellar content — luminosity function — nebulae: planetary

I. INTRODUCTION

Planetary nebulae are potentially one of the best extragalactic standard candles. Bright planetaries are found in galaxies of all Hubble types, can be located in dust-free regions of galaxies, and are best observed through narrow-band filters, which suppress the continuum and simplify the photometry. More importantly, the maximum flux any planetary nebula can emit is governed by the constraints of stellar evolution. If the properties of the brightest planetaries in every galaxy are similar, then with current telescopes and detectors, extragalactic distances up to 20 Mpc can be measured by observing these objects.

Unfortunately, distance determinations for Galactic planetary nebulae are notoriously poor; few Galactic PNs have their distances known to better than 30% (Pottasch 1983). Jacoby (1989; Paper I) has shown, however, that a sharp upper limit to the mass of PN central stars combined with the critical dependence of the evolutionary time scale on central star mass ($\tau \propto M^{-9.5}$), produces an abrupt truncation in the [O III] λ5007 planetary nebula luminosity function (PNLF). Thus, while individual planetary nebulae may be poor primary standard candles, an ensemble of PNs can be an effective distance indicator.

In order to calibrate Jacoby's theoretical PNLF, Ciardullo *et al.* (1989; Paper II) observed several hundred PNs in the bulge of M31. By carefully limiting their analysis to a complete and homogeneous sample of planetaries, Ciardullo *et al.* verified the existence of the high-luminosity cutoff in the PNLF, and proposed an empirical law to describe the luminosity function. Jacoby *et al.* (1989; Paper III), confirmed this relation with an [O III] λ5007 survey of M81's bulge, and showed that the shape of M81's PNLF is identical to both the theoretical curve and the derived distribution in M31. More importantly, Jacoby *et al.* also compared M81's PNLF based distance to distances determined by other methods. The results of this comparison were excellent—the difference between M81's planetary nebulae and *I* band Cepheid distance is an insignificant 7%.

Despite these encouraging results, the true usefulness of PNs for distance determinations is still uncertain. To fully prove the utility of planetary nebulae as standard candles, one more crucial test is required: the PNLF of several galaxies at the same distance, but with different absolute magnitudes, colors, metallicities, and Hubble types must be compared.

The galaxy group in Leo, whose brightest member is NGC 3368 (M96), is the ideal location for performing this comparison. At a distance of $\sim$10 Mpc, it is the closest well-mixed group, containing two giant ellipticals (NGC 3377 and 3379), two SB0s (NGC 3384 and 3412), an Sab (NGC 3368), and an SBb (NGC 3351) all within a 3° × 1°.5 central core. Because the velocity dispersion of this core is small (the galaxies listed above all have radial velocities between $700 < v_{rad} < 900$ km s^{-1}) there is little doubt the galaxies are associated (Turner and Gott 1976; Huchra and Geller 1982; Geller and Huchra 1983; Vennik 1984; Tully 1988). Hence the group is the ideal laboratory for studying the PNLF. The galaxies are close enough so

[1] Visiting Astronomer, Cerro Tololo Inter-American Observatory, National Optical Astronomical Observatories, operated by the Association of Universities for Research in Astronomy, Inc., under contract with the National Science Foundation.

[2] Visiting Astronomer, Kitt Peak National Observatory, National Optical Astronomical Observatories, operated by the Association of Universities for Research in Astronomy, Inc., under contract with the National Science Foundation.

that the PNLF can be well sampled, far enough away so that the finite depth of the cluster is unimportant, and early enough so that samples of planetary nebulae can be identified without the contamination and confusion caused by unresolved H II regions.

Humason, Mayall, and Sandage (1956) first noted that the Leo Cloud's relative proximity makes it an important stepping stone for extragalactic distance measurements. Despite this fact, very few distance estimates to the group exist. Pritchet and van den Bergh (1985) obtained a distance of 6.8 ± 0.8 Mpc from NGC 3379's globular cluster luminosity function, but admitted that the galaxy's specific globular cluster frequency was 1.4 times smaller than that seen in Virgo ellipticals. By modeling the pixel-to-pixel luminosity fluctuations in NGC 3379, Tonry and Schneider (1988) calculated an approximate distance of 9.8 Mpc to the group, but likewise stated that their value depended on a number of assumptions. In a preliminary report based on the Tully-Fisher relationship, Tully and Pierce (1989) derived distances of 9.8 and 10.2 Mpc to the Leo I galaxies NGC 3351 and NGC 3368, but these distances are tied to the calibration of 12 later type spirals. The only other available distance estimator, the elliptical galaxy diameter-velocity dispersion relation (Davies *et al.* 1987; Burstein *et al.* 1987; Lynden-Bell *et al.* 1988), has only been calibrated indirectly in S0 galaxies using the bulges of M31 and M81 (Dressler 1987). When applied to NGC 3377 and NGC 3379, this relation puts Leo I at a distance of 11 Mpc.

In this paper, we will use planetary nebulae to determine accurate distances to three galaxies in the Leo I group—the E0 giant elliptical NGC 3379, its optical companion, the SB0 spiral NGC 3384, and the smaller E6 elliptical NGC 3377. In § II we will describe our observations and briefly review the steps required to extract [O III] λ5007 magnitudes from CCD images. Tables with the positions and magnitudes of the 249 planetaries detected in this group will then be presented. In § III, we will select a complete and homogeneous set of planetaries in each galaxy and show that the luminosity specific PN densities are roughly independent of radius. In § IV, we will use each galaxy's PNLF to determine its most likely distance along with a formal uncertainty. In § V, we will discuss the actual errors in the distances by reviewing possible systematic uncertainties in the photometry and in the assumed extinction. We will conclude by discussing the true shape of the PNLF and the future use of planetary nebulae as distance indicators.

II. OBSERVATIONS AND REDUCTIONS

Over three observing seasons, three galaxies in the core of the Leo I group, NGC 3377, 3379, and 3384, were surveyed for planetary nebulae using the prime focus CCD cameras of the Kitt Peak and Cerro Tololo 4 m telescopes. In 1986 CTIO frames were taken with an RCA CCD, which provided a scale of 0.″6 per pixel, and a field of view of 3′ north-south by 5′ east-west. Observations taken at Kitt Peak in 1987 also used an RCA camera (RCA 3); the scale and field size for these images were identical to that of the CTIO frames, but for this northern data, the chip was oriented with the long direction north-south instead of east-west. In 1988, Kitt Peak's TI 2 CCD was used in the unbinned 800 × 800 pixel mode to produce frames with a scale of 0.″3 per pixel and a field size of 4′ × 4′. The survey regions of each galaxy are displayed in Figure 1 (Plates 14–15).

The observing technique used was similar to that described in Papers II and III. Planetaries were detected through a redshifted [O III] λ5007 filter, with a central wavelength of 5021 Å and a full width half-maximum (FWHM) of 28 Å in the converging beam of the telescopes (cf. § V). A 279 Å wide off-band filter centered at 5290 Å served to define the galaxy continuum. Total on-band exposure times per field were either 5400 or 7200 s, depending on the CCD used and the sky transparency. The off-band exposures were one-eighth as long and went ~0.2 mag fainter than the on-band frames to ensure against the possible misidentification of objects at the frame limit. A log of these observations is presented in Table 1.

Planetaries in the Leo Group were identified and measured in a manner similar to that described in detail in Papers II and III. Because Kitt Peak's RCA 3 CCD has a large radiation event rate, the on-band images from this chip were first cleaned using the IRAF package COSMICRAYS. The multiple on-band and off-band exposures were then aligned and combined in order to create a single [O III] difference frame for each field. This step removed the rapidly varying galaxy background, but left the emission-line sources untouched and greatly simplified the photometric measurements. PN candidates were then located by identifying each field's emission-line sources on the difference frame and confirming their existence on the individual on-band frames. Objects located in regions of field overlap had to be identified in each field, in order to be included in the final object list.

TABLE 1

LEO I GROUP OBSERVATIONS

Galaxy	α(1950)	δ(1950)	UT Date	Telescope	CCD	Number of Frames	Exposure (s)	Seeing (″)
NGC 3379 North	$10^h45^m11^s.5$	12′52″32°	1986 Apr 8	CTIO 4 m	RCA	2	2700	1.4
NGC 3379 South	10 45 11.5	12 48 51	1986 Apr 9	CTIO 4 m	RCA	1	5400	1.5
NGC 3379 East	10 45 18.2	12 50 41	1987 Mar 29	KPNO 4 m	RCA 3	2	2700	2.4
NGC 3379 East	10 45 18.2	12 50 41	1987 Mar 30	KPNO 4 m	RCA 3	1	5400	1.6
NGC 3379 West	10 45 3.2	12 50 40	1987 Mar 30	KPNO 4 m	RCA 3	1	5400	1.8
NGC 3384 East	10 45 46.2	12 53 39	1987 Mar 30	KPNO 4 m	RCA 3	1	5400	1.4
NGC 3377	10 45 3.6	14 14 54	1987 Mar 31	KPNO 4 m	RCA 3	1	5400	1.6
NGC 3384 West	10 45 29.8	12 52 41	1987 Mar 31	KPNO 4 m	RCA 3	1	5400	1.8
NGC 3379 North	10 45 11.1	12 53 10	1988 Apr 9	KPNO 4 m	TI 2	2	2700	1.3
NGC 3379 South	10 45 10.9	12 48 37	1988 Apr 9	KPNO 4 m	TI 2	2	2700	1.1
NGC 3384 North	10 45 39.0	12 55 47	1988 Apr 10	KPNO 4 m	TI 2	2	3600	1.1[a]
NGC 3384 South	10 45 39.4	12 51 22	1988 Apr 10	KPNO 4 m	TI 2	2	3600	1.5[a]
NGC 3377	10 45 3.9	14 14 55	1988 Apr 12	KPNO 4 m	TI 2	2	3600	1.4

[a] Frames taken through light cirrus.

PLATE 14

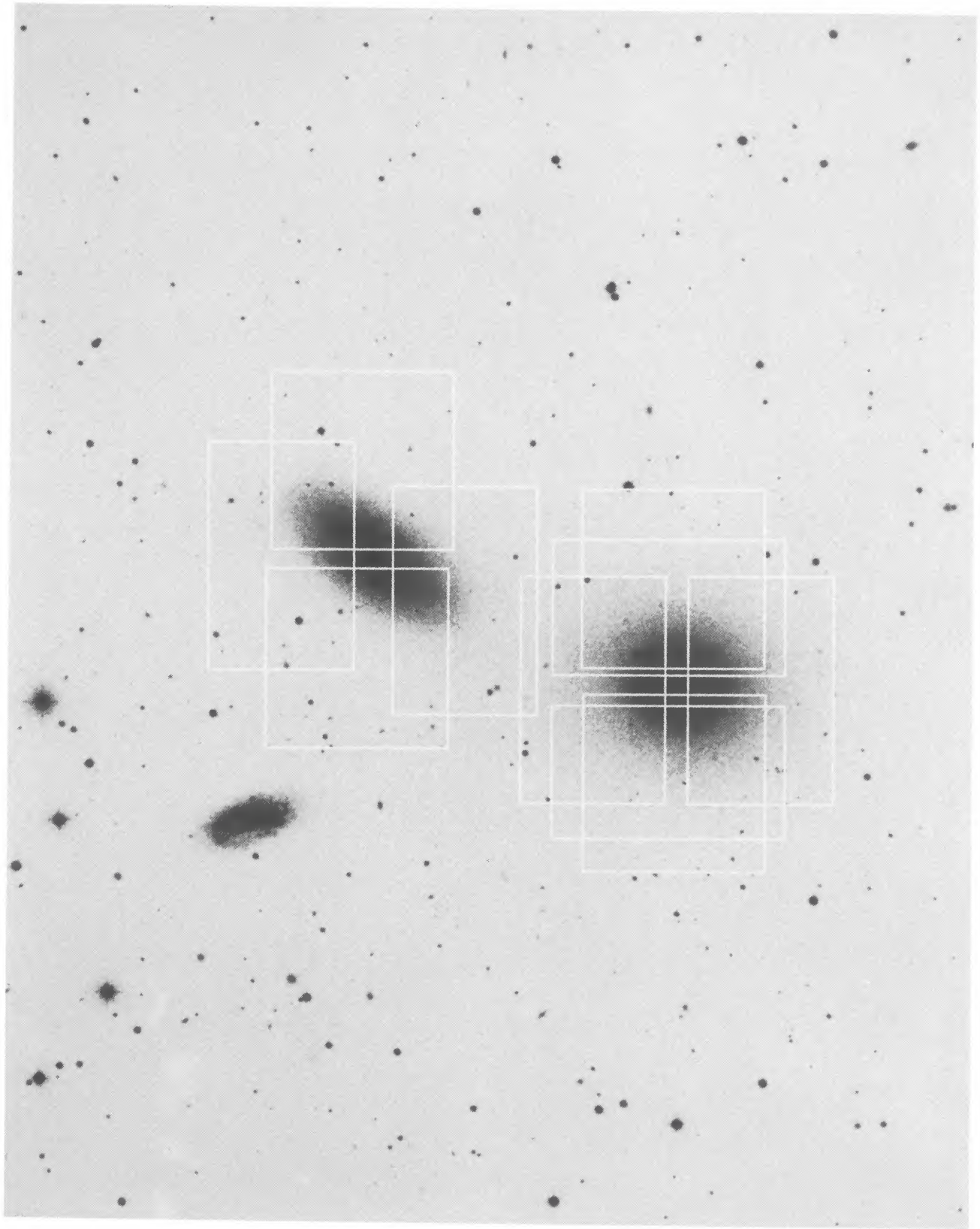

FIG. 1*a*

FIG. 1.—(*a–b*) The 4 m CCD survey fields superposed on a reproduction of a Palomar Sky Survey *E* plate. North is up and east is to the left. Fig. 1*a* shows the noninteracting pair of galaxies NGC 3379 and NGC 3384. NGC 3377, which is two degrees to the north, is shown in Fig. 1*b*. The square regions are those surveyed with the Kitt Peak's TI 2 CCD; the rectangular fields elongated north-south were taken with Kitt Peak's RCA 3 CCD. The two frames of NGC 3379 which were taken at CTIO are the rectangles elongated in the east-west direction.

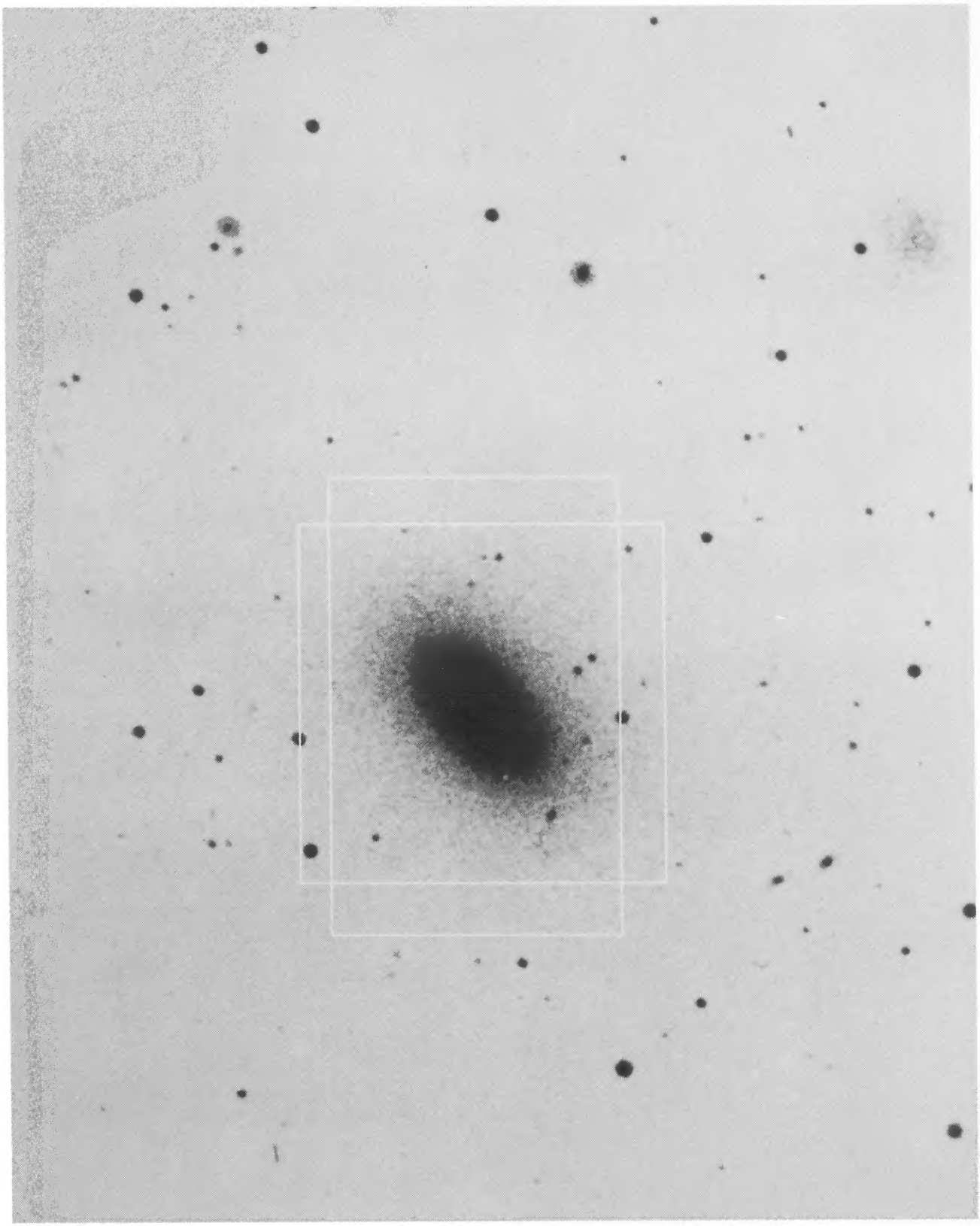

FIG. 1*b*

Since NGC 3377, 3379, and 3384 are all early-type galaxies which contain no obvious star-forming or H II regions, all the stellar [O III] sources found were assumed to be bright planetaries. Faint supernova remnants could, in principle, be confused with bright planetary nebulae; however, such misidentifications in our survey region are unlikely. In the absence of an appreciable interstellar medium, an unimpeded expanding supernova shell should adiabatically cool below detectability in just a few years. (For example, S And 1885, which occurred 15″ from M31's nucleus (cf. de Vaucouleurs and Corwin 1985) was not recovered in Ford and Jacoby's (1978) [O III] λ5007 image-tube survey for bulge planetaries, nor was it seen on Ciardullo *et al.*'s (1988) deep Hα image of M31's bulge.) In any case, since the rate of supernova production in an elliptical galaxy is much less than the rate of planetary nebula formation, misidentified supernova remnants will have a negligible effect on our planetary nebula luminosity function.

After identifying the [O III] λ5007 sources, photometry was performed on all candidate objects and on several comparison stars in the on-band image using the MPC aperture photometry program (Adams *et al.* 1980; Paper III). Since the on-band off-band filter technique enhances the contrast of emission-line sources, virtually all the PN images were isolated and unblended. Hence, for all but the faintest objects, our MPC magnitudes, measured through apertures of the order of the seeing FWHM, should be just as accurate as those which could be obtained via point spread function techniques (cf. Stetson 1987; Paper III).

After calculating raw PN magnitudes, the measurements for each galaxy were placed on a common astrometric and photometric system by taking advantage of the overlap in the CCD fields and using the SUPERPHOT analysis package (Ciardullo *et al.* 1987). The astrometric coordinate system was defined using the positions of several reference stars, as determined from SAO standards measured on the Palomar Sky Survey plates with the Kitt Peak 2 axis Grant engine. Absolute monochromatic fluxes were computed from those frames taken under photometric conditions by comparing the large aperture magnitudes of bright field stars to similar measurements of several spectrophotometric standards (Stone 1977; Oke 1974; Stone and Baldwin 1983). These fluxes were then transformed to [O III] λ5007 absolute magnitudes by modeling the transmission curve of the on-band filter, correcting for the mean transmission at the velocity of the planetaries (Jacoby, Quigley, and Africano 1987; Paper III) and using

$$m_{5007} = -2.5 \log F_{5007} - 13.74 . \quad (1)$$

The multiple measurements of planetaries in the regions of field overlap were used to estimate the random photometric error of these observations.

A list of the PN candidates identified in each galaxy, along with their estimated photometric errors appear in Tables 2–4. From the internal variances of the astrometric solutions, and from the positional residuals of planetaries appearing on multiple frames, we estimate the relative error in the PN equatorial coordinates to be less than 0.″5. The error in the photometric zero point, as derived from the multiple measurements of the photometric standards is ~3%. To facilitate spectroscopic observations, the positions of the reference stars used in the astrometric reductions are given in the Table 5.

III. DEFINING THE SAMPLE

Figure 2 histograms the raw planetary nebula luminosity function observed for the three Leo galaxies. The distributions are remarkably similar. In each galaxy, the brightest planetary nebula has an [O III] magnitude $m_{5007} \approx 25.5$, confirming the utility of these objects as standard candles. At fainter magnitudes, the PNLFs rise rapidly, until incompleteness becomes important at $m_{5007} > 26.5$. No superbright emission objects are seen and, at first glance, there does not appear to be any change in the PNLF with galaxy Hubble type.

Although Figure 2 demonstrates the utility of using planetary nebulae for distance estimates, the displayed data are not statistically complete and homogeneous, and hence cannot be analyzed quantitatively. In addition to the obvious incompleteness at $m_{5007} > 26.5$, PNs brighter than this limit have been missed in regions where the background galaxy lumi-

TABLE 2

NGC 3377 PLANETARY NEBULAE

ID	α(1950)	δ(1950)	N	m_{5007}	s.e.(*m*)	Sample
1.....	10h45m02s95	14°15′11″5	2	25.51	0.09	
2.....	10 45 01.16	14 14 05.6	2	25.60	0.03	S
3.....	10 45 03.31	14 15 10.9	2	25.74	0.15	
4.....	10 45 02.35	14 12 37.8	1	25.81	...	S
5.....	10 45 00.61	14 14 05.3	2	25.84	0.05	S
6.....	10 45 05.22	14 15 17.4	1	25.85	...	
7.....	10 45 09.02	14 16 00.8	2	25.89	0.12	S
8.....	10 45 03.88	14 14 35.6	2	25.90	0.11	
9.....	10 45 07.19	14 15 57.1	2	26.00	0.07	S
10.....	10 45 05.00	14 15 16.8	1	26.06	...	
11.....	10 45 03.84	14 16 30.7	2	26.06	0.07	S
12.....	10 45 03.67	14 14 28.5	2	26.06	0.18	
13.....	10 45 03.45	14 12 43.6	1	26.10	...	S
14.....	10 44 57.35	14 13 17.0	2	26.13	0.17	
15.....	10 45 04.50	14 14 50.0	1	26.13	...	S
16.....	10 45 03.64	14 15 12.9	1	26.15	...	
17.....	10 45 09.91	14 15 35.4	1	26.15	...	S
18.....	10 45 03.62	14 14 35.5	1	26.16	...	
19.....	10 45 02.22	14 15 20.8	2	26.22	0.10	
20.....	10 45 06.38	14 15 13.1	2	26.23	0.10	S
21.....	10 45 00.09	14 14 30.5	2	26.23	0.06	
22.....	10 45 00.81	14 14 05.5	2	26.25	0.25	S
23.....	10 45 01.31	14 16 28.2	2	26.30	0.07	S
24.....	10 45 00.01	14 14 48.3	1	26.35	...	S
25.....	10 45 03.54	14 16 25.1	2	26.38	0.00	S
26.....	10 45 08.71	14 13 32.1	2	26.38	0.29	S
27.....	10 44 58.21	14 14 12.8	2	26.38	0.06	S
28.....	10 45 09.15	14 15 43.9	2	26.39	0.33	S
29.....	10 45 02.78	14 13 56.6	2	26.41	0.17	S
30.....	10 44 59.95	14 14 35.4	2	26.48	0.12	S
31.....	10 45 08.50	14 13 51.0	2	26.48	0.12	S
32.....	10 45 02.14	14 16 09.2	2	26.49	0.15	S
33.....	10 44 58.46	14 13 59.0	2	26.49	0.21	S
34.....	10 45 03.24	14 13 37.5	2	26.54	0.11	
35.....	10 45 01.68	14 14 35.0	2	26.55	0.04	
36.....	10 45 07.90	14 12 50.7	1	26.56	...	
37.....	10 45 04.38	14 14 00.0	2	26.59	0.05	
38.....	10 45 05.64	14 14 58.5	1	26.60	...	
39.....	10 45 08.01	14 14 29.8	1	26.60	...	
40.....	10 45 05.94	14 14 58.5	2	26.61	0.24	
41.....	10 44 59.02	14 14 53.1	1	26.61	...	
42.....	10 44 57.72	14 14 55.1	2	26.63	0.12	
43.....	10 45 07.70	14 14 02.7	2	26.63	0.01	
44.....	10 45 00.38	14 14 59.3	2	26.64	0.21	
45.....	10 45 00.78	14 17 05.5	1	26.65	...	
46.....	10 45 02.90	14 14 18.7	2	26.67	0.19	
47.....	10 44 59.55	14 15 38.1	2	26.74	0.17	
48.....	10 44 59.23	14 13 36.0	1	26.74	...	
49.....	10 45 01.66	14 13 50.1	2	26.76	0.25	
50.....	10 45 04.77	14 14 26.7	2	26.79	0.06	
51.....	10 45 05.29	14 16 03.6	2	26.85	0.12	
52.....	10 45 07.29	14 14 28.6	2	26.88	0.15	
53.....	10 45 01.66	14 14 42.3	1	27.25	...	
54.....	10 45 07.08	14 15 08.0	2	27.51	0.35	

TABLE 3

NGC 3379 PLANETARY NEBULAE

ID	α(1950)	δ(1950)	N	m_{5007}	s.e.(m)	Sample
1	10 45 13.67	12 50 34.4	1	25.28	...	
2	10 45 12.94	12 51 22.0	1	25.33	...	
3	10 45 02.98	12 53 35.6	1	25.44	...	S
4	10 45 10.97	12 50 23.2	1	25.49	...	
5	10 45 12.21	12 51 13.9	1	25.51	...	
6	10 45 13.12	12 51 33.6	3	25.53	0.20	
7	10 45 09.94	12 50 29.3	1	25.63	...	
8	10 45 09.73	12 51 46.4	2	25.65	0.22	S
9	10 45 11.07	12 51 25.5	2	25.66	0.33	
10	10 45 20.77	12 51 01.0	2	25.68	0.08	S
11	10 45 08.76	12 50 53.0	1	25.75	...	
12	10 45 12.58	12 50 52.8	1	25.76	...	
13	10 45 19.42	12 50 09.1	2	25.76	0.07	S
14	10 45 13.83	12 51 29.9	3	25.77	0.15	
15	10 45 22.94	12 50 01.7	2	25.77	0.15	S
16	10 45 13.88	12 51 56.0	3	25.78	0.15	S
17	10 44 59.88	12 50 44.5	1	25.81	...	S
18	10 45 20.42	12 47 46.4	1	25.81	...	S
19	10 45 06.74	12 51 08.0	2	25.83	0.09	
20	10 45 11.50	12 51 30.1	2	25.84	0.02	
21	10 45 03.61	12 48 37.6	3	25.85	0.07	S
22	10 45 17.06	12 50 58.5	2	25.91	0.12	S
23	10 45 13.22	12 50 38.2	1	25.92	...	
24	10 45 15.98	12 49 40.4	1	25.92	...	S
25	10 45 07.77	12 53 57.8	2	25.95	0.06	S
26	10 45 02.01	12 52 29.1	2	25.96	0.07	S
27	10 45 10.52	12 49 31.5	2	25.96	0.14	S
28	10 45 18.39	12 52 04.1	4	25.98	0.23	
29	10 45 06.70	12 50 50.9	1	25.99	...	S
30	10 45 16.37	12 52 15.5	4	26.00	0.09	S
31	10 45 11.59	12 51 12.6	1	26.00	...	
32	10 45 10.40	12 51 41.0	2	26.03	0.10	
33	10 45 10.64	12 51 17.3	2	26.07	0.11	
34	10 45 09.16	12 52 06.7	2	26.07	0.23	S
35	10 45 08.18	12 51 07.0	1	26.09	...	
36	10 45 12.80	12 51 06.0	1	26.10	...	
37	10 45 17.56	12 49 21.1	4	26.13	0.14	S
38	10 45 17.01	12 50 41.5	1	26.14	...	S
39	10 45 18.46	12 51 21.4	2	26.15	0.02	S
40	10 45 07.74	12 49 27.1	3	26.15	0.12	S
41	10 45 04.06	12 51 00.0	1	26.18	...	S
42	10 45 10.59	12 50 19.0	1	26.20	...	
43	10 45 11.47	12 50 12.2	1	26.20	...	
44	10 45 14.98	12 50 32.6	2	26.21	0.22	
45	10 45 00.88	12 50 34.9	1	26.23	...	S
46	10 45 12.47	12 53 08.1	3	26.25	0.12	S
47	10 45 18.74	12 51 54.0	1	26.25	...	S
48	10 45 03.28	12 50 22.3	2	26.26	0.21	S
49	10 45 10.15	12 49 23.2	1	26.28	...	S
50	10 45 07.00	12 49 27.4	3	26.28	0.05	S
51	10 45 16.79	12 49 32.2	3	26.29	0.07	S
52	10 45 14.31	12 52 05.7	3	26.30	0.28	S
53	10 45 08.56	12 52 06.8	1	26.30	...	S
54	10 44 59.55	12 50 48.0	1	26.33	...	S
55	10 45 15.55	12 51 59.9	1	26.33	...	S
56	10 45 12.30	12 50 55.4	1	26.34	...	
57	10 45 17.76	12 49 50.8	1	26.35	...	S
58	10 45 07.99	12 53 48.7	1	26.36	...	
59	10 45 07.76	12 50 00.8	2	26.37	0.66	S
60	10 45 16.70	12 52 07.7	2	26.37	0.12	S
61	10 45 08.55	12 54 20.9	1	26.39	...	S
62	10 45 04.43	12 51 00.6	1	26.40	...	S
63	10 45 07.22	12 50 03.3	3	26.40	0.09	
64	10 45 12.32	12 49 02.6	4	26.42	0.30	S
65	10 45 08.28	12 49 55.2	1	26.43	...	
66	10 45 08.79	12 54 18.0	1	26.44	...	S
67	10 45 17.96	12 47 54.8	1	26.44	...	S
68	10 45 09.05	12 52 08.6	3	26.48	0.48	S
69	10 45 03.02	12 50 15.4	3	26.48	0.04	S
70	10 45 16.08	12 50 27.6	3	26.48	0.32	S
71	10 45 16.23	12 52 47.5	3	26.48	0.37	S
72	10 45 12.51	12 49 04.1	3	26.51	0.14	
73	10 45 15.34	12 50 08.0	1	26.53	...	
74	10 45 09.85	12 48 29.1	2	26.54	0.32	
75	10 45 14.70	12 49 55.8	2	26.56	0.01	
76	10 45 07.38	12 48 38.8	3	26.56	0.16	
77	10 44 57.90	12 49 43.0	1	26.59	...	
78	10 45 12.50	12 49 31.2	3	26.60	0.06	
79	10 45 12.13	12 51 58.6	1	26.64	...	
80	10 45 18.76	12 50 03.9	3	26.67	0.28	
81	10 45 06.45	12 50 49.7	1	26.71	...	
82	10 45 08.21	12 49 43.4	1	26.74	...	
83	10 44 57.48	12 49 40.5	1	26.74	...	
84	10 45 18.31	12 50 00.0	1	26.78	...	
85	10 45 00.23	12 49 15.4	1	26.81	...	
86	10 45 14.99	12 49 52.0	1	26.82	...	
87	10 45 05.76	12 49 25.6	1	26.84	...	
88	10 45 14.56	12 52 23.6	2	26.85	0.07	
89	10 45 16.62	12 51 21.7	1	26.88	...	
90	10 45 05.94	12 49 24.8	1	26.94	...	
91	10 44 57.75	12 51 44.7	1	26.99	...	
92	10 45 05.96	12 50 39.0	1	27.00	...	
93	10 45 03.89	12 53 58.3	1	28.25	...	

nosity is high. Therefore, before any analysis can be performed, a statistically complete sample of PNs must be selected.

There are several ways to estimate how the brightness of the background galaxy affects completeness. The first method, a purely theoretical one, is to calculate the expected signal-to-noise of a PN detection using estimates of the system throughput, the image quality, and the CCD efficiency. Ciardullo *et al.* (1987) and Paper II both used this technique on 0.9 m observations of the bulge and inner disk of M31 to place conservative limits on Hα and λ5007 surveys. In the case of the Leo galaxies, equation (5) of Ciardullo *et al.* (1987) predicts that, for a planetary with $m_{5007} \approx 26.5$, incompleteness should begin to become important (a signal-to-noise less than or equal to 9) where the background surface brightness is $\mu_V \approx 21.8$. In NGC 3377, this occurs $\sim$0.9 from the galaxy's nucleus; in NGC 3379, the theoretical radius of completeness is at an isophotal radius of $\sim$1.2, and in NGC 3384, this distance is $\sim$1.3 from the center. These numbers are only rough estimates, however, since the present survey was performed on two different telescopes, with three different detectors, and through a variety of observing conditions.

A second method of estimating incompleteness, more experi-

TABLE 4

NGC 3384 PLANETARY NEBULAE

ID	α(1950)	δ(1950)	N	m_{5007}	s.e.(m)	Sample	ID	α(1950)	δ(1950)	N	m_{5007}	s.e.(m)	Sample
1	10 45 46.03	12 54 35.3	2	25.59	0.10	S	52	10 45 38.02	12 52 35.9	1	26.40	...	S
2	10 45 34.35	12 52 44.9	2	25.63	0.13	S	53	10 45 42.50	12 53 58.0	2	26.41	0.26	
3	10 45 36.44	12 53 17.5	1	25.66	...		54	10 45 46.33	12 52 36.9	2	26.42	0.20	S
4	10 45 38.63	12 54 18.9	1	25.67	...		55	10 45 43.00	12 54 11.5	2	26.42	0.17	S
5	10 45 39.15	12 53 59.7	1	25.71	...		56	10 45 32.00	12 52 44.8	1	26.43	...	S
6	10 45 33.43	12 53 12.3	2	25.73	0.24	S	57	10 45 39.08	12 53 01.7	1	26.44	...	
7	10 45 33.14	12 53 24.1	1	25.81	...	S	58	10 45 34.58	12 51 45.6	2	26.45	0.13	S
8	10 45 33.52	12 52 18.1	2	25.85	0.14	S	59	10 45 35.88	12 52 55.3	1	26.45	...	
9	10 45 35.24	12 52 37.3	1	25.86	...	S	60	10 45 33.41	12 53 12.2	1	26.46	...	S
10	10 45 31.15	12 53 27.6	1	25.90	...	S	61	10 45 42.48	12 53 08.6	1	26.49	...	S
11	10 45 46.78	12 55 28.3	2	25.93	0.21	S	62	10 45 48.07	12 54 55.8	1	26.49	...	S
12	10 45 34.96	12 53 58.3	2	25.94	0.04	S	63	10 45 38.98	12 54 26.3	1	26.51	...	
13	10 45 45.75	12 51 27.9	2	25.95	0.01		64	10 45 24.31	12 52 54.0	1	26.54	...	
14	10 45 35.03	12 52 53.1	1	25.96	...	S	65	10 45 43.82	12 55 40.4	2	26.54	0.12	
15	10 45 26.63	12 53 13.0	1	25.97	...	S	66	10 45 44.41	12 54 30.4	2	26.55	0.14	
16	10 45 40.17	12 54 10.6	2	25.98	0.15		67	10 45 34.83	12 53 50.5	2	26.56	0.18	
17	10 45 42.42	12 54 14.6	1	25.99	...		68	10 45 33.79	12 52 43.6	2	26.58	0.28	
18	10 45 38.43	12 53 11.9	1	25.99	...		69	10 45 43.13	12 53 26.3	1	26.59	...	
19	10 45 42.33	12 54 13.8	1	26.01	...		70	10 45 33.02	12 53 07.2	2	26.60	0.23	
20	10 45 42.08	12 54 45.6	2	26.04	0.08	S	71	10 45 44.12	12 54 07.4	1	26.61	...	
21	10 45 30.56	12 53 35.3	1	26.05	...	S	72	10 45 40.48	12 53 56.3	1	26.61	...	
22	10 45 39.69	12 52 28.3	1	26.06	...	S	73	10 45 35.50	12 51 52.6	1	26.62	...	
23	10 45 36.74	12 52 01.4	1	26.06	...	S	74	10 45 38.34	12 52 43.6	1	26.63	...	
24	10 45 37.65	12 53 54.4	1	26.07	...		75	10 45 37.27	12 52 31.1	1	26.68	...	
25	10 45 42.41	12 54 30.9	2	26.09	0.10	S	76	10 45 34.47	12 52 26.7	2	26.69	0.25	
26	10 45 40.60	12 53 51.4	2	26.10	0.20		77	10 45 33.24	12 53 58.3	2	26.70	0.09	
27	10 45 45.57	12 54 17.0	2	26.11	0.10	S	78	10 45 48.56	12 56 00.3	1	26.70	...	
28	10 45 35.07	12 53 01.5	2	26.11	0.18		79	10 45 46.53	12 55 36.0	2	26.70	0.05	
29	10 45 40.26	12 55 53.9	2	26.11	0.09	S	80	10 45 32.06	12 50 31.5	1	26.72	...	
30	10 45 33.68	12 52 49.8	2	26.14	0.05	S	81	10 45 32.75	12 53 01.3	2	26.73	0.35	
31	10 45 32.02	12 53 15.1	2	26.16	0.01	S	82	10 45 39.82	12 54 16.4	1	26.73	...	
32	10 45 33.67	12 52 49.7	2	26.16	0.08	S	83	10 45 42.43	12 53 21.0	1	26.73	...	
33	10 45 38.06	12 54 02.0	1	26.18	...		84	10 45 32.57	12 52 07.1	2	26.75	0.32	
34	10 45 37.70	12 53 08.4	1	26.20	...		85	10 45 41.20	12 55 06.3	2	26.76	0.07	
35	10 45 41.06	12 53 21.1	1	26.21	...	S	86	10 45 43.32	12 55 15.7	2	26.80	0.06	
36	10 45 30.00	12 53 17.1	1	26.21	...	S	87	10 45 36.41	12 54 09.2	1	26.80	...	
37	10 45 35.90	12 52 39.1	2	26.30	0.11	S	88	10 45 43.15	12 51 58.2	1	26.81	...	
38	10 45 38.30	12 54 31.7	1	26.30	...	S	89	10 45 25.77	12 54 06.9	1	26.83	...	
39	10 45 34.64	12 52 34.7	2	26.31	0.00	S	90	10 45 36.24	12 54 24.1	1	26.84	...	
40	10 45 41.29	12 54 07.5	2	26.31	0.08		91	10 45 36.46	12 53 58.6	1	26.89	...	
41	10 45 42.04	12 54 03.8	2	26.32	0.11		92	10 45 42.60	12 56 59.8	1	26.95	...	
42	10 45 34.89	12 51 08.4	1	26.33	...	S	93	10 45 40.69	12 52 49.2	2	26.96	0.00	
43	10 45 34.79	12 53 43.1	1	26.34	...	S	94	10 45 36.68	12 53 59.9	1	26.96	...	
44	10 45 41.34	12 52 35.8	2	26.35	0.03	S	95	10 45 38.02	12 54 45.4	1	26.97	...	
45	10 45 51.29	12 54 27.9	1	26.35	...	S	96	10 45 37.26	12 56 02.4	1	27.06	...	
46	10 45 34.82	12 53 53.4	2	26.36	0.09	S	97	10 45 41.14	12 53 57.0	2	27.15	0.11	
47	10 45 45.18	12 54 05.7	2	26.36	0.10	S	98	10 45 31.50	12 57 10.5	1	27.18	...	
48	10 45 42.04	12 53 32.8	1	26.36	...	S	99	10 45 36.62	12 54 10.6	1	27.22	...	
49	10 45 43.22	12 54 35.7	2	26.38	0.14	S	100	10 45 51.98	12 55 40.7	1	27.24	...	
50	10 45 40.82	12 53 23.1	1	26.38	...		101	10 45 43.63	12 54 20.1	1	27.30	...	
51	10 45 26.77	12 51 37.1	1	26.39	...	S	102	10 45 49.53	12 53 47.5	1	27.42	...	

mental in nature, was detailed in Paper III. By randomly placing artificial stars on a CCD frame of M81's bulge and then "observing" these objects, lower limits to the PN completeness in that galaxy were calculated. Unfortunately, this type of experiment is extremely time consuming, and requires the independent analysis of every CCD field. Since, in the case of the Leo galaxies, we are more concerned with the net completeness for an entire galaxy, rather than the results of any individual field, such an analysis seemed unwarranted.

The most efficient method of determining the incompleteness in a sample of planetaries is through an empirical examination of the data. As pointed out in Paper II, stellar evolution theory predicts that the number of planetaries per unit galaxy luminosity does not change much with either the age or the initial mass function of a stellar population (Renzini and Buzzoni 1986). Observations of M31's bulge and inner disk confirm this (Paper II) and show that the spatial distribution of PNs in that galaxy closely follows the luminosity profile. A

TABLE 5

LEO I ASTROMETRIC REFERENCE STARS

Galaxy	ID	α(1950)	δ(1950)
NGC 3377.....	a	$10^h45^m11^s.56$	14°14′41″.3
	b	10 45 11.11	14 13 27.4
	c	10 45 08.20	14 13 35.4
	d	10 44 56.98	14 14 52.3
	e	10 44 58.30	14 15 31.4
	f	10 44 58.97	14 15 23.5
	g	10 45 04.79	14 16 09.1
NGC 3379.....	a	10 45 22.17	12 52 55.9
	b	10 45 19.56	12 53 04.5
	c	10 45 03.43	12 53 37.2
	d	10 45 00.86	12 52 47.0
	e	10 45 15.07	12 51 26.5
	f	10 45 05.98	12 53 35.3
	g	10 45 04.52	12 49 07.8
	h	10 45 05.88	12 47 30.9
	i	10 45 01.88	12 48 06.3
	j	10 44 58.32	12 49 40.2
	k	10 44 57.46	12 50 31.9
	l	10 45 15.79	12 49 53.0
	m	10 45 06.70	12 46 54.8
	n	10 45 11.97	12 54 58.4
	o	10 45 09.82	12 46 43.0
	p	10 45 00.73	12 50 19.3
	q	10 45 01.87	12 51 13.4
	r	10 45 20.06	12 52 25.3
	s	10 45 01.88	12 51 45.4
NGC 3384.....	a	10 45 40.30	12 52 29.9
	b	10 45 41.71	12 52 24.3
	c	10 45 33.03	12 52 56.6
	d	10 45 42.47	12 55 13.7
	e	10 45 44.51	12 55 12.8
	f	10 45 41.91	12 56 06.5
	g	10 45 35.22	12 54 32.6
	h	10 45 51.44	12 54 51.9
	i	10 45 48.77	12 55 00.9
	j	10 45 48.67	12 54 49.5
	k	10 45 34.60	12 53 27.5
	l	10 45 46.55	12 57 10.6
	m	10 45 25.98	12 53 35.6
	n	10 45 31.85	12 56 48.2
	o	10 45 44.42	12 50 24.9
	p	10 45 43.17	12 49 39.1
	q	10 45 33.59	12 50 19.1
	r	10 45 42.40	12 51 42.7

direct method of examining the completeness is therefore to measure the luminosity specific PN number density as a function of background surface brightness. For late-type galaxies which have spiral arms, dust lanes, and irregular luminosity contours, such a comparison is difficult. However, for smooth elliptical and S0 galaxies, the measurement is straightforward.

The three Leo galaxies were each modeled using a series of concentric elliptical isophotes with varying axial ratios and position angles. For NGC 3377, the surface photometry and ellipticities were taken from Peletier *et al.* (1988); for NGC 3379, the photometric data was that of de Vaucouleurs and Capaccioli (1979), and for NGC 3384, the model used was that of Barbon, Capaccioli, and Tarenghi (1975) and Barbon, Benacchio, and Capaccioli (1976). The isophotal radial distance of each planetary from the center of its parent galaxy was then calculated by finding the semimajor axis of the isophote upon which it was superposed. The distribution of these distances was compared to the luminosity profile along the galaxy's major axis, corrected for the fraction of light enclosed in the survey regions.

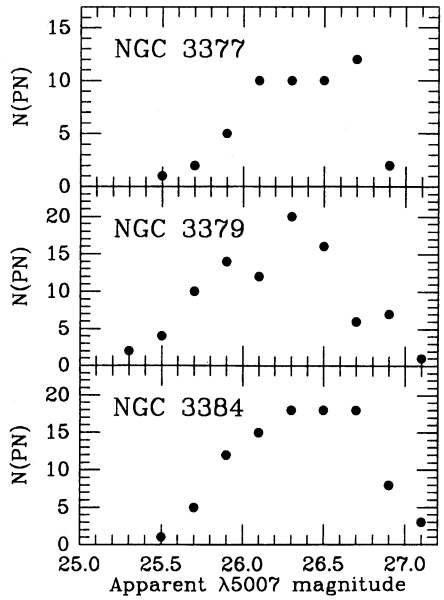

FIG. 2.—The raw planetary nebula luminosity functions in NGC 3377, 3379, and 3384 binned into intervals of 0.2 mag. Although heterogeneous, the samples demonstrate the similarity of the PNLF in galaxies of differing Hubble types. From the magnitudes of the brightest PNs, all three galaxies appear to be at approximately the same distance, with NGC 3379 being the closest. The decrease in the number of planetaries with $m_{5007} > 26.5$ is due to incompleteness.

Figure 3 performs this comparison using planetaries brighter than the nominal completeness limit of $m_{5007} = 26.5$. As expected, at large radii the PN spatial distribution agrees very closely with the luminosity profile. However, near the galactic centers, where the bright background luminosity is rapidly

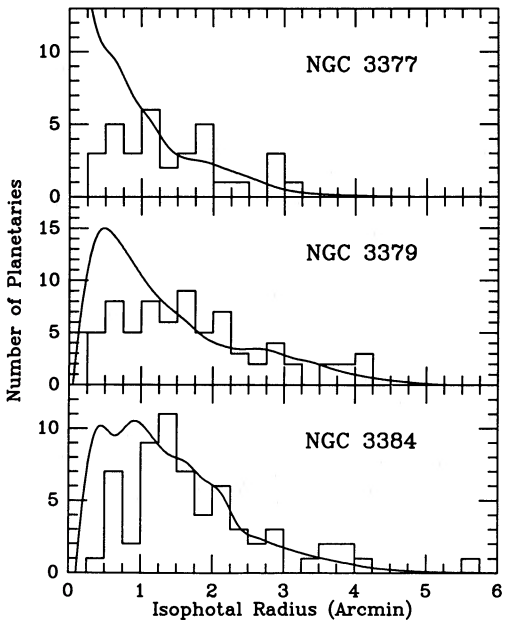

FIG. 3.—Three histograms showing the distribution of isophotal radii for PN candidates with $m_{5007} < 26.5$. The solid lines display the amount of B luminosity surveyed in each galaxy. A comparison of these curves with the data shows that in the inner regions of the galaxies, incompleteness is important, as PNs are being lost amid the bright background. In the outer areas, however, no significant gradient in the luminosity specific PN density is seen.

TABLE 6

SUMMARY FOR LEO I GALAXIES

Parameter	NGC 3377	NGC 3379	NGC 3384
Galaxy type (RSA)	E6	E0	$SB0_1(5)$
B_T (RSA)	11.10	10.33	10.70
Systemic velocity (km s^{-1})	718	893	771
$(B-V)_T^0$ (RC2)	0.79	0.89	0.84
Assumed A_{5007}	0.05	0.04	0.06
$B_{\rm sampled}$	12.76	11.64	12.21
$m_{\rm bol}$	11.14	9.83	10.46
PN magnitude completeness limit	26.5	26.5	26.5
Inner isophotal radius for sample	60″	75″	75″
Maximum background surface brightness	22.0	21.9	21.7
Total number of PNs found	54	93	102
Number of PNs in complete sample	22	45	43
Most likely distance modulus (μ_0)	30.07	29.96	30.03
Most likely distance (Mpc)	10.3	9.8	10.1
Most likely specific PN density ($\alpha_{2.5}$)	37×10^{-9}	21×10^{-9}	38×10^{-9}
Implied stellar death rate	1.5×10^{-11}	8.5×10^{-12}	1.5×10^{-11}

varying, the faintest planetaries are lost, and the apparent specific PN density drops sharply. This fall-off can be used to estimate incompleteness. For example, in NGC 3384, planetaries with $m_{5007} < 26.5$ are obviously lost within 75″ of the nucleus, where the background surface brightness is $\mu_V < 21.7$. Outside this region, the sample appears relatively complete: a Kolmogorov-Smirnov (K-S) test on the two distributions shows no evidence for a radial gradient in the luminosity specific PN density. A similar statement can be made for NGC 3377 and 3379. In NGC 3377, PNs with $m_{5007} < 26.5$ appear complete to within 1′ of the nucleus, or until the background surface brightness exceeds $\mu_V \sim 22.0$. In NGC 3379, the apparent specific PN density remains constant to within $\sim 75''$ from the nucleus, where $\mu_V \sim 21.9$. These limits and regions are summarized in Table 6. Those planetaries in Tables 2–4 which are members of the statistical samples are identified with an "S."

IV. THE PNLF COMPARISON AND THE DISTANCE TO LEO

The best way to translate a complete sample of PN magnitudes into a distance determination is to treat the PNLF as a probability distribution and assume the observations are drawn randomly from this function. From Papers II and III, a good representation of the PNLF, in terms of the magnitude scale defined by equation (1), is

$$N(M) \propto e^{0.307M}[1 - e^{3(M^*-M)}], \quad (2)$$

where $M^* = -4.48$. Thus, by adopting the magnitude completeness limits implied by Figure 2, and fitting the observations to the empirical curve, extragalactic distances can quickly be derived.

Unfortunately, although this procedure seems straightforward, in practice several additional parameters must be taken into account. The first is the relation describing the photometric error versus magnitude. Although the true PNLF may be constant from galaxy to galaxy, the observed luminosity function is always a convolution of the true function and the observational error profile. Hence, to properly fit our data to a predicted curve, an estimate for the measurement error is needed. Fortunately, this can be derived from the PN magnitudes. In general, the signal-to-noise of an observation depends on both the object's flux and the background surface brightness. However, in the case of our Leo observations, the latter term dominates only in regions where incompleteness is important. Since these regions are excluded from the analysis anyway, the photometric error is, to a good approximation, parameterized solely by magnitude. Those planetaries in our statistical sample with multiple measurements were therefore binned into 0.2 mag intervals and the within class variance was calculated for each bin. This error function was then plotted for each galaxy. As expected, because the three galaxies were observed in parallel and had similar PN completeness limits, no significant differences in the relations were found. The data for the three galaxies were therefore combined and a smooth curve fitted through the points. This resulting function, tabulated in Table 7, defines the expected standard error versus magnitude.

The second quantity needed for a distance determination is an estimate of the interstellar extinction affecting the [O III] λ5007 magnitudes. Because the galaxies involved are all of very early type, internal extinction in these objects is expected to be small. However, despite being at a high galactic latitude ($b \approx 57°$) the foreground extinction to Leo may not be negligible. Global reddening estimates all give very low values: the formulae of Sandage (1973), Burstein and McDonald (1975), and de Vaucouleurs, de Vaucouleurs, and Corwin (1976; RC2) yield $E(B-V)$ values of 0.0, 0.039, and 0.047, respectively, while the reddening maps of Burstein and Heiles (1982) show no evidence of extinction. Although at the moment there is no way of knowing the precise amount of reddening in front of each galaxy, as a best guess, we adopted the Burstein and Heiles (1984) values obtained from their 21 cm H I observations. These B magnitude extinctions were transformed to total

TABLE 7

PN PHOTOMETRIC ERROR VERSUS MAGNITUDE

Magnitude	Number of PNs with Multiple Measurements	Mean 1 σ Error (Observed)	Mean 1 σ Error (Adopted)
25.6	5	0.11	0.11
25.8	8	0.12	0.12
26.0	14	0.12	0.125
26.2	17	0.13	0.13
26.4	24	0.19	0.15
26.6	18	0.17	0.17
26.8	11	0.17	0.19

extinctions at redshifted λ5007 using Seaton's (1979) expression for extinction as a function of wavelength. The resulting A_{5007} values are listed in Table 6.

With the magnitude completeness limit, the photometric error function, and interstellar extinction known, the distance to each galaxy can be solved directly using the maximum likelihood expressions in Paper II. Before doing so, however, one additional quantity should be calculated. As a by-product of the PNLF fitting procedure, the total number of planetaries in each system is also found. By normalizing this number to the total amount of bolometric luminosity surveyed, it is possible to make a direct comparison between the PN observations and stellar population theory.

To perform this normalization, the surface photometry of Peletier *et al.* (1988), de Vaucouleurs and Capaccioli (1979), Barbon, Bennacchio, and Capaccioli (1976), and Barbon, Cappacioli, and Tarenghi (1975) were used to compute the total B luminosity encompassed in each survey region. From these B luminosities, dereddened V magnitudes were calculated using the colors and transformations of Sandage and Visvanathan (1978*a*) and the Galactic extinction values of Burstein and Heiles (1984). Next, the bolometric correction appropriate for each galaxy was estimated. This was done by first dereddening the raw *UBVRJHK* colors by Perrson, Frogel, and Aaronson (1979) and then comparing the derived bolometric fluxes to those found for a library of stellar spectra (Paper II). The resulting bolometric corrections were then used to compute the total bolometric magnitude of each survey region. These are listed in Table 6.

Figure 4 plots the maximum likelihood solutions to fits of the PNLF using probability contours spaced at 0.5 σ intervals. The abscissa displays the true distance modulus implied by the fits; the ordinate gives the derived bolometric luminosity specific density of planetaries within 2.5 mag of M^*. Immediately obvious is the agreement in the distances derived for all three galaxies. As summarized in Table 6, despite having different Hubble types, colors, and absolute magnitudes, the most likely distance moduli for the galaxies differ by only 0.11 mag. This scatter, which translates into $\sim$500 kpc, is less than the depth of a typical cluster, and demonstrates the power of planetary nebulae as distance indicators. Just as striking, however, are the small error contours associated with the solutions. The 1 σ error contours for NGC 3379 and 3384 are only $\sim$0.12 mag wide, an uncertainty which corresponds to a distance error of $\pm$6%. Because fewer planetaries were detected in NGC 3377, the error contours for this galaxy are slightly larger (1 $\sigma \approx$ 0.18 mag), but this $\pm$9% error is still acceptable. The mean distance to the group, 10 Mpc, is in excellent agreement with that derived from the Tully-Fisher relation (Tully and Pierce 1989) and agrees well the distances derived from the luminosity fluctuation method (Tonry and Schneider 1988) and the diameter-velocity dispersion relationship (Davies *et al.* 1987; Burstein *et al.* 1987; Dressler 1987). It does not, however, agree with the distance derived from NGC 3379's globular clusters (Pritchet and van den Bergh 1985).

A second feature of the probability contours is the agreement in $\alpha_{2.5}$, the luminosity specific number density of planetaries within 2.5 mag of M^*. The most probable value for the PN density of NGC 3377 is exactly the same as that derived for NGC 3384, and, although the value for NGC 3379 is slightly lower, the confidence contours for all three galaxies overlap enough so that a single value for the group is not excluded. Considering the errors involved in estimating the galactic bolometric magnitudes this is good agreement. Furthermore, if the most likely value for $\alpha_{2.5}$ found in NGC 3377 and 3384 is extrapolated over the entire 8 mag of the planetary nebula luminosity function via equation (2), then a typical PN lifetime of 25,000 yr (Pottasch 1984) implies a luminosity specific stellar death rate of $\sim 1.5 \times 10^{-11}$ stars yr^{-1} $L_\odot{}^{-1}$. Remarkably, this is within 30% of the theoretical death rate of $\sim 2 \times 10^{-11}$ stars yr^{-1} $L_\odot{}^{-1}$ derived by Renzini and Buzzoni (1986) for an old stellar population. Again, considering the extrapolations involved and the uncertainties in relating the rate of PN formation to the stellar death rate, this agreement is exceptional. The stellar death rates derived for M31 and M81 were both slightly lower than expected from theory and could have been affected by internal extinction in the galactic bulges (Papers II and III). The agreement between the theoretical stellar death rate and the values determined from the early-type Leo galaxies yields strong support for the form of the PNLF used as well as the interpretation that the detected emission-line objects are indeed all planetary nebulae.

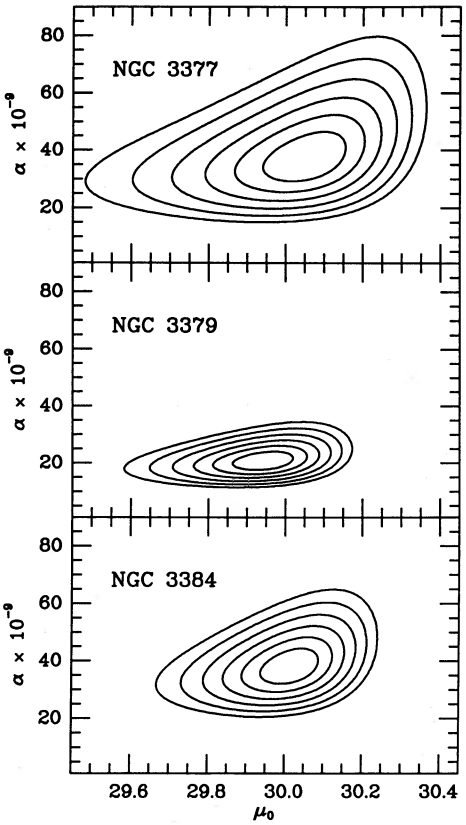

FIG. 4.—Maximum likelihood confidence contours for NGC 3377, 3379, and 3384 derived from complete and homogeneous samples of PNs in each galaxy and assuming the empirical PNLF of eq. (2). The abscissa is the true distance modulus μ_0; the ordinate is the number of planetaries within 2.5 mag of M^* normalized to the amount of bolometric luminosity sampled. Contours are drawn at 0.5 σ intervals. The extinctions listed in Table 6 have been applied. The best-fit solutions for the three galaxies have μ_0 = 30.07, 29.96, and 30.03, respectively.

The small error contours associated with the maximum likelihood solutions suggest that the empirical PNLF is a good fit to the observed data. However, the fits do not prove the model used is an appropriate one, nor do they test whether the luminosity functions of the three galaxies have significant differences. Such tests are straightforward, however.

Figure 5 compares the observed PNLFs derived from the complete samples of planetaries found in the three Leo galaxies. The solid lines display the empirical law translated to the most likely galactic distances and convolved with the photometric error function. Small number statistics create some scatter in the diagrams, particularly in the small elliptical NGC 3377, but the fits are clearly acceptable. For each galaxy, a K-S test shows an overwhelming acceptance of the hypothesis that the PNs are indeed drawn from the universal PNLF. In NGC 3377, the cumulative probability function derived from its 22 planetaries deviates from the model by 0.15, a number which is much less than the 20% rejection statistic of 0.22. For NGC 3379 and 3384, which have 45 and 43 PNs in their statistical samples, the numbers are even better: the observed differences of 0.09 and 0.11 are much smaller than the 20% rejection statistic of 0.16. Two sample K-S tests between the PN luminosity distributions of each galaxy show just as good agreement. From these tests, we conclude that the shape of the PNLF within each of these early-type galaxies is the same, and this shape agrees with the empirical model derived from M31 and M81.

Another way to demonstrate the agreement between the observed PNLF in Leo and theory is to combine the planetary nebula data from all three galaxies and compare the resulting magnitude distribution with the theoretical PNLF derived in Paper I. This is done in Figure 6, which displays both luminosity functions in log space. Once again, the match to the observations is exceptional. The PNLF is not a power law, and the rapid cutoff at the bright end of the PNLF is dramatic. It is this cutoff which makes the PNLF such an effective distance indicator.

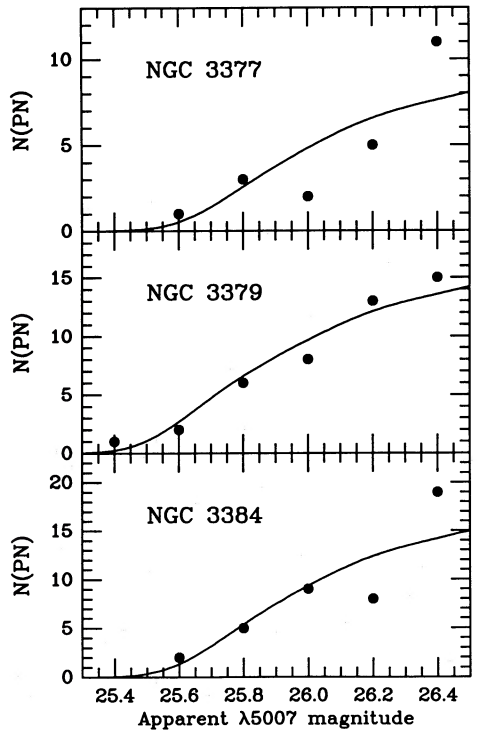

FIG. 5.—The observed PNLF in NGC 3377, 3379, and 3384 derived from homogeneous and complete samples of planetaries. The data have been binned into 0.2 mag intervals. The solid lines show the empirical PNLF convolved with the mean photometric error vs. magnitude relation and translated by the most likely apparent distance moduli.

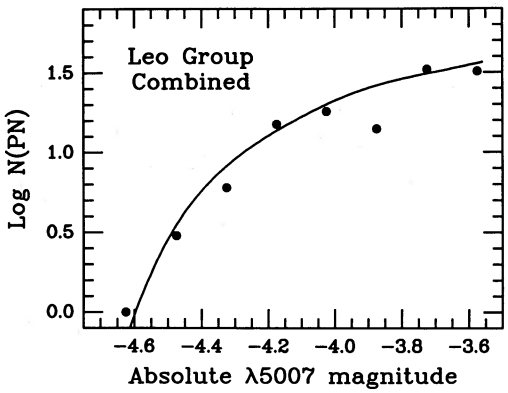

FIG. 6.—A log plot of the combined Leo I PNLF derived from a complete and homogeneous sample of planetaries. The data have been binned into 0.15 mag intervals and transformed to absolute magnitude using the extinctions and most likely distance moduli of Table 6. The solid line is the theoretical PNLF computed in Paper I convolved with the mean photometric error vs. magnitude relation. As has been noted about the PNLFs of M31 and M81 the agreement between observations and theory is exceptional.

V. UNCERTAINTIES

Despite the small formal errors in the PNLF maximum likelihood solutions, the actual uncertainties in the distance measurements are somewhat larger. Errors in the photometry and uncertainties about the underlying physics both introduce systematic errors which are larger than the random noise included in the statistics. While the uncertainties in the physical assumptions can only be estimated qualitatively, the effects of measurement errors can be quantitatively investigated.

Because our PNLF fitting procedure allows for measurement error, the effects of random uncertainties in the PN magnitudes are included in the maximum likelihood solution. Systematic errors in the photometric zero points, of course are not, and, while the SUPERPHOT analysis package does insure that each field within a galaxy is on the same relative system, it does rely on an external calibration to set the zero point. Systematic deviations may therefore exist due to errors in the aperture corrections, in the filter transmissions, and in the spectrophotometric calibration.

To maximize the photometric accuracy, the raw magnitudes were measured with apertures close to the seeing FWHM. To put the measurements on an absolute system, these results were scaled by an aperture correction, found by comparing large-aperture and small-aperture magnitudes of bright field stars. Typically, each CCD field contained two or three stars suitable for this purpose, which defined an aperture correction to $\sim 2\%$. Because systematic errors between galaxy fields were removed by forcing the magnitudes of objects in the overlap regions to match, the effective uncertainty in the aperture corrections is somewhat less than this, $\sim 1.5\%$.

A second source of systematic error is in the flux calibration. In order to determine the system sensitivity at 5007 Å, nine flux standards, EG 50, EG 63, EG 67, Feige 34, Ross 640, Kopff 27, BD $+8°2015$, BD $+33°2642$, and LTT 6248, were observed during the course of the survey, with at least two standard star observations on each photometric night. (EG 54 was also observed regularly, but compared to the other standards, the star consistently appeared too bright by ~ 0.13 mag.) By using the mean atmospheric extinction coefficients for Kitt Peak (Barnes and Hayes 1984) and CTIO (Stone and Baldwin 1983) the standards were placed at the same airmasses as the Leo I

frames and a direct comparison of the relative fluxes was performed. On any night, the scatter in the derived flux constants was ~3%, with a ~2% error of the mean. Again, the true uncertainty in the flux calibration is probably less than this, since frames calibrated on different nights have been tied together through the measurement of objects in overlapping fields.

An additional uncertainty in the derived fluxes comes about because of the wide shoulders of the λ5007 filter's transmission curve. Because spectrophotometric standards are continuum objects, a proper flux calibration for emission line sources requires knowledge of this curve. If the transmission is constant over the width of the filter, the sensitivity function for the two types of objects is the same; if the transmission varies, the mean sensitivity derived from standard stars must be scaled to the monochromatic transmission at the emission line (Jacoby, Quigley, and Africano 1987).

The redshift λ5007 filter used for observing the Leo galaxies has a boxlike transmission curve in parallel light with negligible wings. However, because the f/2.77 beam of the 4 m prime focus contains ray angles between 4°.3 (set by the secondary mirror obscuration) and 10°.2, the true sensitivity function for the filter is much broader. Following Paper III, we modeled the filter transmission curve by interpolating and integrating over laboratory spectrophotometer measurements, which were taken in nearly parallel light with tilt angles between 0° and 11°. We then checked this result using reimaging optics in the KPNO coudé feed spectrograph. Our model for the f/2.77 beam transmission appears in Figure 7, along with the measured transmission in parallel light. The bandpass of the model agrees with that measured at the coudé feed to better than 3%, and in the region near peak transmission, the predicted and observed filter curves are virtually identical.

Figure 7 also shows the systemic velocities of the Leo galaxies. The redshifts of these three galaxies place [O III] λ5007 near the peak of the filter transmission curve; however, due to the finite velocity dispersions within the galaxies, the exact transmission applicable to any individual planetary is unknown. For example, in NGC 3379, the combination of galactic rotation and random stellar motion creates an observed dispersion of ~150 km s^{-1} at a distance ~1′ from the nucleus (Davies and Illingworth 1983). From Figure 7, this translates directly into an asymmetric flux error of ~4%. In order to minimize this uncertainty, we used the observed velocity dispersions of Davies and Illingworth (1983), Davies *et al.* (1987), and Tonry and Davis (1981) to calculate velocity weighted mean filter transmissions for each galaxy. However, because the error is asymmetric, systematic errors in the residuals remain. In theory, we could have removed this effect with an appropriate modeling of the observational error in the maximum likelihood procedure (Paper II); however in the case of the three Leo galaxies, this second order uncertainty is negligible.

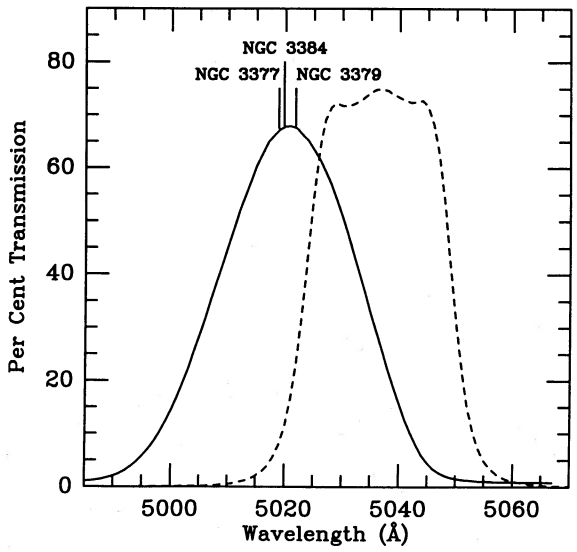

FIG. 7.—The transmission curves for the [O III] λ5007 filter used in this survey. The dashed line represents the filter transmission in parallel light in the laboratory. The solid line is a model for the transmission at 11°C in an f/2.77 beam with a 4°.3 central obstruction. The systemic velocities of the three Leo galaxies are marked.

The above discussion implies a total systematic uncertainty in the Leo group distances of ~4%. This is, of course, in addition to the formal error found for M31, upon which the calibration is based (Paper II). This leads to a total uncertainty of ~11%, not counting the errors in the individual fits of § IV.

Unfortunately, the largest uncertainty in the derived Leo I distances is not due to any error in the photometry, but instead arises from the unknown interstellar extinction. As detailed in § IV, the H I observations of Burstein and Heiles (1984) yield total extinctions of $A_{5007} \approx 0.05$ mag. Other extinction estimates do exist, however, which range from 0 (Sandage 1973) to 0.17 (RC2). These numbers alone indicate an uncertainty of ~8%. (Our preliminary distance to Leo I [Ciardullo, Jacoby, and Ford 1988; Jacoby, Ciardullo, and Ford 1988; Paper I) assumed the RC2 extinction of 0.17, and is thus ~7% smaller than the value presented here.) While in principle the reddening toward each of these galaxies can be estimated by measuring the Hα to Hβ ratio of the brightest PNs, this observation must wait for a larger telescope. Until then, this additional uncertainty cannot be removed, and it will affect all extragalactic distance measurements made at optical wavelengths.

VI. PLANETARY NEBULAE AS DISTANCE INDICATORS

The most serious question concerning planetary nebulae concerns the relationship between the PNLF and the underlying stellar population. Because planetaries are part of the latest stages of stellar evolution, their evolution is poorly understood. If the planetary nebula luminosity function changes drastically with either age or metallicity, then it is possible that PN based distances will have large systematic errors. Fortunately, this does not appear to be the case.

A number of different physical processes tend to buffer the variation of [O III] λ5007 flux with stellar population. For example, there is some evidence from the UV fluxes of elliptical galaxies (Burstein *et al.* 1988) and from stellar evolution theory (Bertelli, Chiosi, and Bertola 1989) that the mass of a PN central star (and therefore its peak [O III] luminosity) varies inversely with metallicity. An examination of the λ5007 fluxes from the brightest PNs in the Local Group (Paper II) lends support to this idea—despite their small mass, the metal-poor Magellanic Clouds contain some of the brightest planetaries in the system. However, although a decrease in the metal abundance may result in an increase in a PN central star's UV flux, this same decrease will also lower the efficiency of forbidden line cooling by removing metals from the nebula. Thus, the effect of metallicity is moderated—despite a factor of 10 difference in the abundances observed in Local Group galaxies, the fluxes of the brightest PNs vary by less than 40%.

The best evidence for the invariance of PN [O III] emission, however, comes from the Leo group galaxies. NGC 3377 and 3379 are both normal ellipticals with Hubbles types E6 and E0, respectively. According to the RSA catalog (Sandage and Tammann 1981) NGC 3379 is brighter than NGC 3377 by ~ 1.3 mag, and, from the Mg_2 spectroscopic index of Terlevich *et al.* (1981), the galaxy is also more metal-rich by ~ 0.1 [Fe/H]. NGC 3384 is classified as an SB0 by the RSA catalog, and, although its metallicity has never been estimated, its magnitude and color are intermediate between that of the two ellipticals (Sandage and Visvanathan 1978*b*; Persson, Frogel, and Aaronson 1979). Together the three galaxies represent a fair range in luminosity and metal abundance. The PNLF of each galaxy, however, is identical—not only is the shape of the luminosity function the same for each object, but the derived distances place all three galaxies well within the nominal ~ 1 Mpc region expected for a typical galaxy cluster. This invariance is the best evidence to date for the utility of planetaries as standard candles for early-type galaxies.

Papers I and II demonstrated both theoretically and empirically that the planetary nebula luminosity function is not a power law—there is an apparent upper limit to a planetary's [O III] λ5007 luminosity, and a knee ~ 0.7 mag fainter than this limit. When it is possible to sample the top ~ 1 mag of the luminosity function, distances can be found reliably by the maximum likelihood procedures described in Paper II. However, for the most distant galaxies, only a few of the very brightest planetaries may be visible. Thus, it is important to know whether there are any super-bright planetaries, or, put another way, do any planetaries exist with [O III] magnitudes brighter than M^*.

As discussed in Paper I, a planetary nebula's maximum [O III] λ5007 luminosity depends strongly on the mass of its central star, and since the evolutionary time scale of the star goes inversely as a high power of its mass ($M^{-9.5}$), the probability of finding a high-mass central star at its brightest is very small. However, the evidence from M31, M81, NGC 5128 (Ford *et al.* 1988), and the three Leo galaxies suggests that the probability of finding a PN with $M < M^*$ is *very, very*, small. In those six galaxies, no planetary has yet been found to have an [O III] luminosity greater than the observed limit, M^*. Thus, it is possible that, in fact, the probability of this occurring is truly zero. Paper I discussed several possible reasons for the absence of [O III] bright PNs, including the possibility that the evolutionary time scales for the most massive central stars ($M > 0.75\ M_\odot$) are so fast that, while the central star is bright, the nebula density never drops below the critical value for collisional de-excitation of the forbidden lines. (An example of such a nebula may be the [O III] weak PN SMC23 [Boroson and Liebert 1989]). In any case, at the present time, the evidence suggests that the maximum magnitude cutoff in the PNLF is absolute. If this is true, then Jacoby and Lesser's (1981) assumption that an upper limit to the distance of any galaxy can be derived from the detection of just one planetary is correct.

This work was supported in part by NASA grants NAS 529293 and NAGW-421.

REFERENCES

Adams, M., Christian, C., Mould, J., Stryker, L., and Tody, D. 1980, *Stellar Magnitudes from Digital Pictures* (Tucson: Kitt Peak National Observatory).
Barbon, R., Benacchio, L., and Capaccioli, M. 1976, *Astr. Ap.*, **51**, 25.
Barbon, R., Capaccioli, M., and Tarenghi, M., 1975, *Astr. Ap.*, **38**, 315.
Barnes, J. V., and Hayes, D. S. 1984, in *IRS Standard Star Manual* (Tucson: Kitt Peak National Observatory).
Bertelli, G., Chiosi, C., and Bertola, F. 1989, *Ap. J.*, **339**, 889.
Boroson, T. A., and Liebert, J. 1989, *Ap. J.*, **339**, 844.
Burstein, D., Bertola, F., Buson, L. M., Faber, S. M., Lauer, T. R. 1988, *Ap. J.*, **328**, 440.
Burstein, D., Davies, R. L., Dressler, A., Faber, S. M., Stone, R. P. S., Lynden-Bell, D., Terlevich, R. J., and Wegner, G. 1987, *Ap. J. Suppl.*, **64**, 601.
Burstein, D., and Heiles, C. 1982, *A.J.*, **87**, 1165.
———. 1984, *Ap. J. Suppl.*, **54**, 33.
Burstein, D., and McDonald, L. H. 1975, *A.J.*, **80**, 17.
Ciardullo, R., Ford, H. C., Neill, J. D., Jacoby, G. H., and Shafter, A. W. 1987, *Ap. J.*, **318**, 520.
Ciardullo, R., Jacoby, G. H., and Ford, H. C. 1988, *The Extragalactic Distance Scale*, ed. S. van den Bergh and C. J. Pritchet (A.S.P. Conference Series No. 4) (Provo: Brigham Young University Press), p. 203.
Ciardullo, R., Jacoby, G. H., Ford, H. C., and Neill, J. D. 1989, *Ap. J.*, **339**, 53 (Paper II).
Ciardullo, R., Rubin, V. C., Jacoby, G. H., Ford, H. C., and Ford, W. K., Jr. 1988, *A.J.*, **95**, 438.
Davies, R. L., Burstein, D., Dressler, A., Faber, S. M., Lynden-Bell, D., Terlevich, R. J., and Wegner, G. 1987, *Ap. J. Suppl.*, **64**, 581.
Davies, R. L., and Illingworth, G. 1983, *Ap. J.*, **266**, 516.
de Vaucouleurs, G., and Capaccioli, M. 1979, *Ap. J. Suppl.*, **40**, 699.
de Vaucouleurs, G., and Corwin, H. G., Jr. 1985, *Ap. J.*, **295**, 287.
de Vaucouleurs, G., de Vaucouleurs, A., and Corwin, H. J., Jr. 1976, *Second Reference Catalog of Bright Galaxies* (Austin: University of Texas Press) (RC2).
Dressler, A. 1987, *Ap. J.*, **317**, 1.
Ford, H. C., Ciardullo, R., Jacoby, G. H., and Hui, X. 1988, in *IAU Symposium 131, Planetary Nebulae*, ed. S. Torres-Peimbert (Dordrecht: Reidel), p. 335.
Ford, H. C., and Jacoby, G. 1978, *Ap. J. Suppl.*, **38**, 351.
Geller, M. J., and Huchra, J. P. 1983, *Ap. J. Suppl.*, **52**, 61.
Huchra, J. P., and Geller, M. J. 1982, *Ap. J.*, **257**, 423.
Humason, M. L., Mayall, N. U., and Sandage, A. R. 1956, *A.J.*, **61**, 97.
Jacoby, G. H. 1989, *Ap. J.*, **339**, 39 (Paper I).
Jacoby, G. H., Ciardullo, R., Ford, H. C., and Booth, J. 1989, *Ap. J.*, **344**, 704.
Jacoby, G. H., Ciardullo, R., and Ford, H. C. 1988, in *The Extragalactic Distance Scale*, ed. S. van den Bergh and C. J. Pritchet, A.S.P. Conference Series No. 4 (Provo: Brigham Young University Press), p. 42.
Jacoby, G. H., and Lesser, M. P. 1981, *A.J.*, **86**, 185.
Jacoby, G. H., Quigley, R. J., and Africano, J. L. 1987, *Pub. A.S.P.*, **99**, 672.
Lynden-Bell, D., Faber, S. M., Burstein, D., Davies, R. L., Dressler, A., Terlevich, R. J., and Wegner, G. 1988, *Ap. J.*, **326**, 19.
Oke, J. B. 1974, *Ap. J. Suppl.*, **27**, 21.
Peletier, R. F., Davies, R. L., Illingworth, G. D., Davies, L. E., and Cawson, M. C. M. 1988, in preparation.
Persson, S. E., Frogel, J. A., and Aaronson, M. 1979, *Ap. J. Suppl.*, **39**, 61.
Pottasch, S. R. 1983, in *IAU Symposium 103, Planetary Nebulae*, ed. D. R. Flower (Dordrecht: Reidel), p. 391.
Pottasch, S. R. 1984, *Planetary Nebulae: A Study of Late Stages of Stellar Evolution* (Dordrecht: Reidel), p. 215.
Pritchet, C. J., and van den Bergh, S. 1985, *A.J.*, **90**, 2027.
Renzini, A., and Buzzoni, A. 1986, in *Spectral Evolution of Galaxies*, ed. C. Chiosi and A. Renzini (Dordrecht: Reidel), p. 195.
Sandage, A. 1973, *Ap. J.*, **183**, 711.
Sandage, A., and Tammann, G. A. 1981, *A Revised Shapley-Ames Catalog of Bright Galaxies* (Washington: Carnegie Institution of Washington) (RSA).
Sandage, A., and Visvanathan, N. 1978*a*, *Ap. J.*, **223**, 707.
Sandage, A., and Visvanathan, N. 1978*b*, *Ap. J.*, **225**, 742.
Seaton, M. J. 1979, *M.N.R.A.S.*, **187**, 73P.
Stetson, P. B. 1987, *Pub. A.S.P.*, **99**, 191.
Stone, R. P. S. 1977, *Ap. J.*, **218**, 767.
Stone, R. P. S., and Baldwin, J. A. 1983, *M.N.R.A.S.*, **204**, 347.
Terlevich, R., Davies, R. L., Faber, S. M., and Burstein, D. 1981, *M.N.R.A.S.*, **196**, 381.
Tonry, J. L., and Davis, M. 1981, *Ap. J.*, **246**, 666.
Tonry, J., and Schneider, D. P. 1988, *A.J.*, **96**, 807.
Tully, R. B. 1988, *Nearby Galaxies Catalog* (Cambridge: Cambridge University Press).
Tully, B., and Pierce, M. 1989, private communication.
Turner, E. L., and Gott, J. R. 1976, *Ap. J. Suppl.*, **32**, 409.
Vennik, J. 1984, *Tartu Astr. Obs., Teated*, **73**, 3.

ROBIN CIARDULLO and GEORGE H. JACOBY: Kitt Peak National Observatory, P.O. Box 26732, Tucson, AZ 85726

HOLLAND C. FORD: Space Telescope Science Institute, 3700 San Martin Drive, Baltimore, MD 21218